

APPLICATION OF FAST MULTIPOLE METHOD TO MICROMAGNETIC SIMULATION OF PERIODIC SYSTEMS

D. M. Apalkov and P. B. Visscher¹

(1) Dept. of Physics and MINT Center, University of Alabama, Tuscaloosa, AL 35487-0324

Abstract—We have developed a new method for computing the magnetostatic field of an infinite array of images of an arbitrary system of charges or multipoles. The result takes the form of a Taylor expansion of the potential of a “cored array” of distant images, as is required by the fast multipole method, the most efficient method known for calculating magnetostatic fields in very large systems. The new method is much faster and simpler to implement than the usual Ewald summation or fast Fourier transform, and does not require a regular grid inside the central cell.

Index Terms—Fast Multipole Method, long-range interaction, micromagnetics, periodic boundary conditions.

I. INTRODUCTION

The most time-consuming part of a micromagnetic calculation is the computation of the magnetostatic field at each computational cell due to each of the other cells. Straightforward calculation requires a time of order N^2 , where N is the number of cells. Recently fast multipole methods (FMM) have been introduced [1], [2] that reduce this time to order N . However, there has previously been no simple way to apply the FMM to periodic systems, such as thin films or nanoparticle arrays. The potential of an infinite array of copies of a system can be calculated (in the FMM as well as in other methods) using the Ewald summation method [3], [4], or by solving the Poisson equation by fast Fourier transform [5], but both of these methods are quite complicated and require a regular grid. In this paper we introduce a new iterative method for calculating the fields of the periodic images, which is simpler and more in the spirit of the FMM. In fact, since an FMM code already has functions for convoluting multipoles [2], the present method requires very little additional coding.

II. PERIODIC BOUNDARY CONDITIONS IN THE FMM

In Fig. 1, we show an infinite periodic system, consisting of a central square cell (heavy lines) and infinitely many

identical copies of this cell on a square lattice, of which eight are shown in Fig. 1. These are the cells whose centers lie within a chosen radius R of the origin; charge within these near images is taken into account directly by the FMM method [2]. To account for more distant images, we require a Taylor expansion about the origin (well convergent within the central cell) of their potential. This is obtained from a multipole expansion, replacing the charges in each image by a point multipole at the image center (the points marked “1” in Fig. 1, which form a “cored” infinite square array).

Because the errors in the multipole expansion of order n decrease as R^{-n-1} , the potential can be obtained quite accurately within the central cell with $R/(\text{cell size})$ not much larger than the value 1.7 we use for illustration here. It is actually sufficient to compute the field of a cored periodic array of point charges, since the field of any multipole can be expressed as a derivative of this [2].

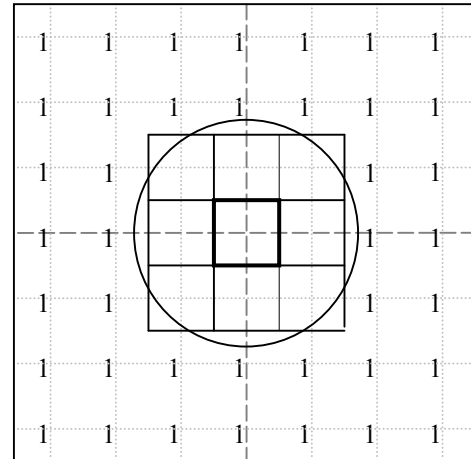


Fig. 1. “Cored” infinite square array of unit charges. Only 9 images are shown, as solid squares. The dashed squares are not images, but the dashed grid connects the centers of images, labeled by “1”. The figure shows 2D system or 2D projection of 3D system.

III. ITERATIVE CALCULATION OF CORED-ARRAY POTENTIAL

We will denote the charge distribution of the cored array of unit charges in Fig. 1 by

$$q_{\mathbf{r}}^{\text{cored}} = \begin{cases} 1 & \text{if } |\mathbf{r}| > R \text{ and } |\mathbf{r}| < R_{\text{cut}}, \\ 0 & \text{otherwise} \end{cases}, \quad (1)$$

where the components of the lattice vector \mathbf{r} are multiples of the lattice spacings a_x, a_y, a_z . [For simplicity, we assume here a cubic lattice but the method works just as well if the a 's are different.] We have introduced a cutoff radius R_{cut} to prevent the divergence of the Coulomb potential

$$V^{\text{cored}}(\mathbf{r}) = \frac{1}{4\pi} \sum_{\mathbf{r}'} \frac{q_{\mathbf{r}'}^{\text{cored}}}{|\mathbf{r} - \mathbf{r}'|}. \quad (2)$$

We will show that this divergence does not affect the fields, which approach definite limits as $R_{\text{cut}} \rightarrow \infty$. We will calculate this potential of the cored charge distribution by a self-similarity argument: it is equivalent to knowing the potential $V^{\text{coarse}}(\mathbf{r})$ of a coarse array with twice the lattice spacing, $q_{2\mathbf{r}}^{\text{coarse}} = q_{\mathbf{r}}^{\text{cored}}$, shown in Fig. 2(a). But we can reconstruct the fine-scale array by convoluting the coarse one with a function $w(\mathbf{t})$ that replaces each coarse charge by a weighted combination of 27 charges [9 in the 2D representation in Fig. 2(b)] using $w(\mathbf{t}) = 2^{-|t_x|} 2^{-|t_y|} 2^{-|t_z|}$, with each $t_i = -1, 0, \text{ or } 1$. Then the convolution $w * q^{\text{coarse}}$ [shown in Fig. 2(c)] almost gives back the fine cored array; the difference

$$q_{\mathbf{r}}^{\text{shell}} \equiv q_{\mathbf{r}}^{\text{cored}} - \sum_{\mathbf{t}} w(\mathbf{t}) q_{\mathbf{r}-\mathbf{t}}^{\text{coarse}} \quad (3)$$

is nonzero only in a shell approximately between radii R and $2R$, as shown in Fig. 3, as well as in a thin shell near the cutoff radius R_{cut} . Defining the potentials of the other charge distributions by equations similar to Eq. (2) above, and substituting the $q_{\mathbf{r}}^{\text{cored}}$ obtained from Eq. (3) into Eq. (2), we obtain

$$V^{\text{cored}}(\mathbf{r}) = V^{\text{shell}}(\mathbf{r}) + \sum_{\mathbf{t}} w(\mathbf{t}) V^{\text{coarse}}(\mathbf{r} - \mathbf{t}). \quad (4)$$

From this equation we can calculate the cored potential iteratively, rescaling the new cored potential to give the coarse potential:

$$V^{\text{coarse}}(2\mathbf{r}) = \frac{1}{2} V^{\text{cored}}(\mathbf{r}). \quad (5)$$

In the fast multipole method [2], what we actually need is a Taylor expansion of the potential at the origin,

$$V^{\text{cored}}(\mathbf{r}) = \sum_{\mathbf{n}} \frac{1}{n_x! n_y! n_z!} V_{\mathbf{n}}^{\text{cored}} x^{n_x} y^{n_y} z^{n_z}. \quad (6)$$

However, it is not hard to show that the real-space convolution in (4) becomes a convolution on the integer-vector Taylor expansion index \mathbf{n} :

$$V_{\mathbf{n}}^{\text{cored}} = V_{\mathbf{n}}^{\text{shell}} + \sum_{\mathbf{p}} w_{\mathbf{p}} V_{\mathbf{n}+\mathbf{p}}^{\text{coarse}}. \quad (7)$$

Here $w_{\mathbf{p}}$ is the multipole moment of $w(\mathbf{t})$, considered as a charge distribution:

$$w_{\mathbf{p}} = \sum_{\mathbf{t}} \frac{1}{p_x! p_y! p_z!} w(\mathbf{t}) t_x^{p_x} t_y^{p_y} t_z^{p_z}. \quad (8)$$

It is Eq. (7) that we actually use in the computation of the cored potential. All of the Taylor coefficients with order $\mathbf{n} \neq \mathbf{0}$ have finite limits as the cutoff $R_{\text{cut}} \rightarrow \infty$. The divergent coefficient $V_{\mathbf{0}}^{\text{coarse}}$ appears only in the equation for the divergent $V_{\mathbf{0}}^{\text{cored}}$, which we need never use. In this limit, the effects of the thin shell near the cutoff on $V_{\mathbf{n}}^{\text{shell}}$ vanish, and we need only include the charges shown explicitly in Fig. 3.

What makes this method so appealing is that it involves very little programming beyond what is already necessary to do an FMM calculation. We already have a function that calculates the Taylor expansion of the field of a point charge at an arbitrary point [2], which allows us to calculate $V_{\mathbf{n}}^{\text{shell}}$. The rescaling that gives the coarse potential (Eq. 5) can be

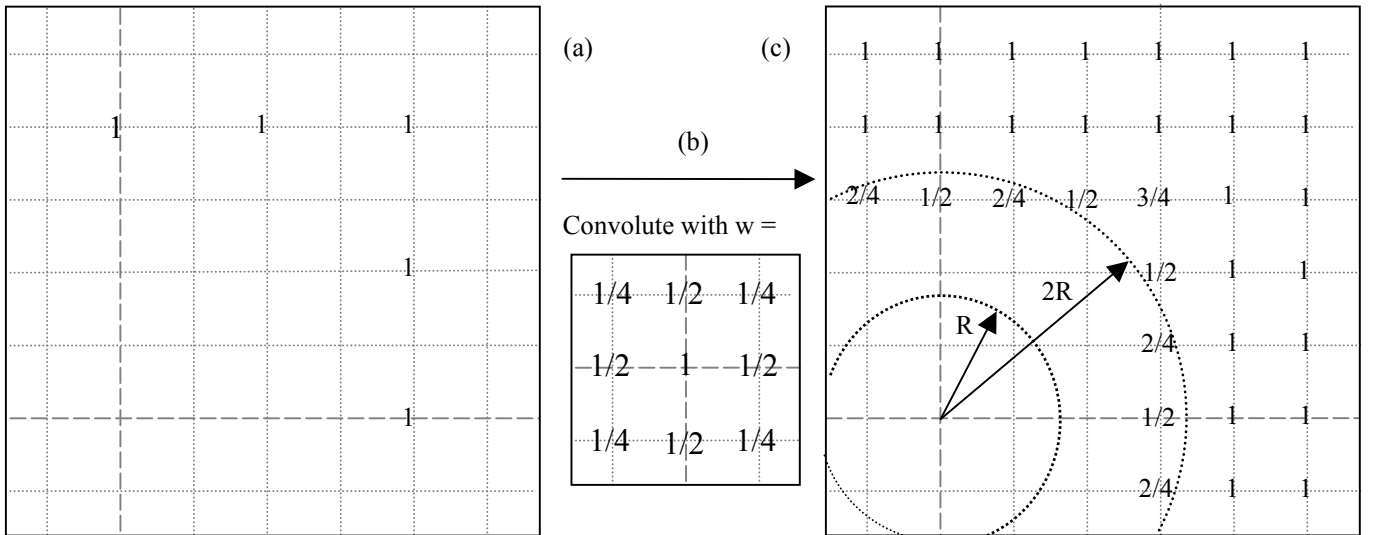


Fig. 2. Superposition of translated copies of the coarse array of unit charges (a) with different translations (b) gives a fine array of charges (c), similar to Fig. 1 except for the shell roughly between the two circles. Only one quadrant is shown, because of symmetry.

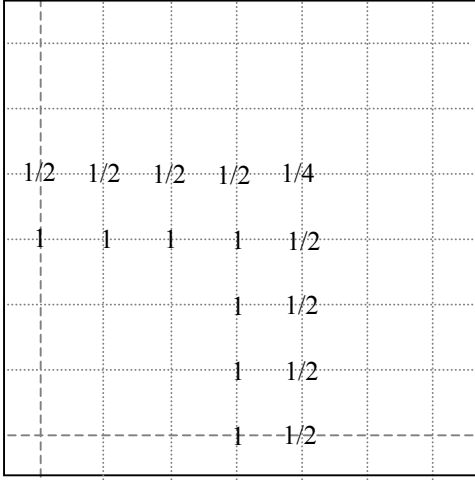


Fig. 3. Point charges of “shell” correction, q^{shell} .

written in terms of Taylor coefficients as

$$V_{\mathbf{n}}^{\text{coarse}} = 2^{-n_x - n_y - n_z - 1} V_{\mathbf{n}}^{\text{cored}}. \quad (9)$$

Thus by alternately using Eq. (7) and Eq. (9), we converge on the correct cored potential. This computation requires a negligible amount of time, since it is done only once and converges rapidly (8 iterations give 5 figure accuracy). To understand why this iteration converges, it is useful to note that any error in the cored potential is pushed twice as far from the origin by the rescaling (Eq. 5) at each iteration, and eventually recedes to infinity.

IV. RESULTS

To demonstrate that the cored-array method is an efficient way to deal with distant charges, we present some visualizations of the potential of the cored array of point charges. Figure 4 shows the potential in a plane through the

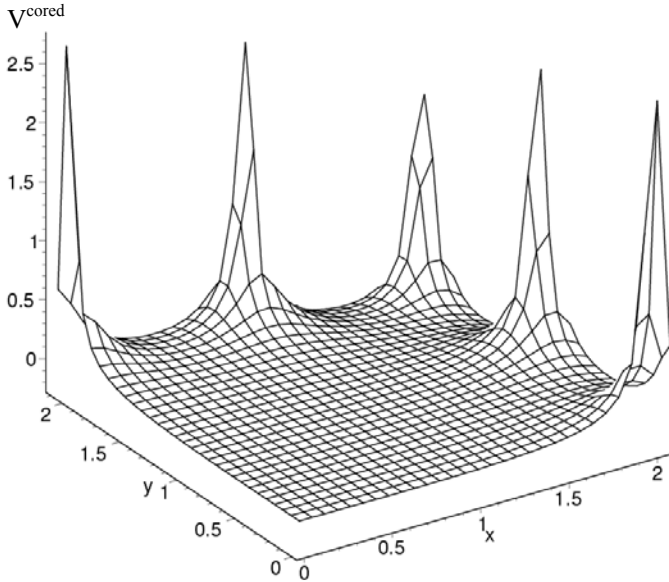


Fig. 4. 3D plot of the potential of the cored array of unit point charges (Fig. 1), in the xy plane. Spikes at $x=2$ and $y=2$ show the positions of the point charges (distances are in units of the periodicity a .)

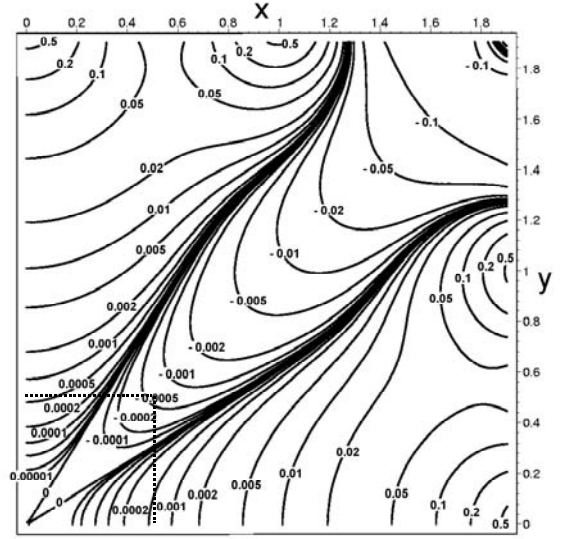


Fig. 5. Contour plot of the cored-array potential. Note that the contour intervals are nearly logarithmic. The square at the origin represents the boundaries of the central image of the system.

origin (the plane of Figs. 1-3). Note that the potential is extremely flat in the central image of the system (the square bounded by $x, y = \pm 0.5$) which is actually used in a micro-magnetic calculation. One way to understand this flatness is to note that the cored array is a discrete approximation to a spherically symmetric charge distribution, whose field would be exactly zero in the central cavity.

To display the potential more quantitatively in the flat region, we show in Fig. 5 a contour plot of the same quadrant, with roughly logarithmically spaced contours. The potential is given relative to its value at the origin, so the origin is on a $V=0$ contour; because of the logarithmic spacing, contours bunch up near this $V=0$ contour and it appears elsewhere as a very thick contour (for example near the charge at $(2,2,0)$). Within the central image, the potential is given very accurately by the Taylor expansion (6), which is explicitly

$$V^{\text{cored}}(x, y, z) = \frac{0.110572}{4!} (2x^4 + 2y^4 + 2z^4 - 6x^2y^2 - 6y^2z^2 - 6z^2x^2) + \frac{0.0219011}{6!} (2x^6 + 2y^6 + 2z^6 - 15x^4y^2 - 15y^4z^2 - 15z^4x^2 - 15x^2y^4 - 15y^2z^4 - 15z^2x^4 + 180x^2y^2z^2) + O(r^8).$$

We have checked this result against direct summation of Eq. (2) with cutoff radius $R_{\text{cut}}=7a$, and find that the contour plots are almost identical inside the root cell. We have also computed the value at the corner $(0.5, 0.5, 0.0)$ to greater accuracy ($R_{\text{cut}}=30a$) and find 5.88×10^{-4} , which differs from the iterative result by only 1.05×10^{-6} . Although this error is in the potential of an array of point charges, this is the worst-case scenario for an actual system – potentials of higher-order multipoles will converge even more rapidly.

REFERENCES

- [1] L. Greengard and V. Rokhlin, *J. Comp. Phys.* **73**, 325-348 (1987).

- [2] P. B. Visscher and D. M. Apalkov, "Simple recursive Cartesian implementation of fast multipole algorithm", preprint at bama.ua.edu/~visscher/mumag/cart.pdf.
- [3] M. P. Allen and D. J. Tildesley, *Computer Simulation of Liquids*, Clarendon Press, 1987, p. 156.
- [4] A. Y. Toukmaji, J. A. Board Jr., "Ewald summation techniques in perspective: a survey", *Comp. Phys. Commun.*, **95**, 73-92 (1996).
- [5] R. Ferré, "Large scale micromagnetic calculations for finite and infinite 3D ferromagnetic systems using FFT", *Comp. Phys. Commun.*, **105**, 169-186 (1997).